GIS-Based Spatial Analysis of River Setback Policy Violations and Flood Vulnerability Along River Ngadda in Maiduguri, Nigeria

***Mustapha Shettima[1,2]., Garba Hassan Sambo.[2], Ali Garga Bukar[3], Ali Mai Boyoma[1] and Yakaka Mustapha[1]**

[1]Department of Environmental Science, Integral University Lucknow, India

[2]Department of Geography, University of Maiduguri, Borno State

[3]Department of Civil and Water Resources Engineering, University of Maiduguri

DOI: https://doi.org/10.51583/IJLTEMAS.2026.1502000006

Received: 13 February 2026; Accepted: 18 February 2026; Published: 23 February 2026

ABSTRACT

This paper evaluates riparian buffer zone violations and examine its consequences on the building-level flood vulnerability along River Ngadda in Maiduguri, northeastern Nigeria. Geographic Information Systems (GIS) was used to integrate high-resolution satellite images and building footprint data in order to determine structures in the river channel. The channel was digitized on full tank level and subdivided into five sections (A-E) in which graduated buffer zones of 10m, 20m and 30m which corresponding to Nigerian planning setback requirements- were generated. Spatial overlay analysis was used to measure encroachment extent and density along the river corridor, while building vulnerability was classified using distance-based proximity and summarized through a Vulnerability Index (VI, a weighted index of proportional exposure to flood risk). Spatial autocorrelation was used to determine patterns of clustering on a segment basis. Findings indicate a large encroachment of 3,065 buildings in the 30m buffer, of which 716 were in the most vulnerable 0-10m area. The VI values were 1.73-1.90 which showed moderate to high flood risk, and central urban segments were most vulnerable.

The spatial analysis revealed mostly negative autocorrelation indicating fragmented and not clustered vulnerability likely reflecting incoherent informal encroachment. Comparative analysis of distance-based vulnerability and building density showed complementary data, whereby single-proxy measures could be a poor fitting characterization of risk. The results indicate that the river could have been less effective in flood attenuation capacity due to weak setback enforcement which was worsened by the excessive solid waste disposal which diminished the conveyance of the channels. The management suggestions are based on spatially oriented intervention: phased relocation of highest-risk structures in central segments, prohibition of the emergence of new communities, clearing of channels and waste management plans, and institutional reinforcement. Preventive management is essential in peripheral segments and expansion needs to be stopped before weakness is diminished.

Keywords: Urban flooding, Riparian buffer zones, Setback violation, Flood vulnerability, Spatial analysis, River Ngadda

INTRODUCTION

Urban flooding is one of the most central environmental issues in the sub-Saharan African region due to the significant growth in the frequency of flood disasters in the past several decades (Manandhar et al., 2023; Nkwunonwo et al., 2016). It is estimated that urban centers in the area will increase three times by 2050, which will only increase the burden on the environment and flood risks (UN-Habitat, 2020; Guneralp et al., 2017). Nigeria, the most populous country in Africa, has experienced devastating floods that have claimed thousands of lives, displaced thousands of people, and destroyed billions of nairas of infrastructure (Umar & Gray, 2023).

ISSN 2278-2540 | DOI: 10.51583/IJLTEMAS | Volume XV, Issue II, February 2026

Maiduguri becomes one of the most flood-prone cities in northeastern Nigeria to floods, where the River Ngadda serves as the main city drainage channel (Uba, 2024; Obroh & Sambo, 2022).

River Ngadda, a tributary of the Lake Chad Basin, traverses the middle of Maiduguri and has traditionally been a source of important ecosystem services, such as supplying water, flood management, groundwater replenishment, and nutrient cycling (Sanyaolu, et al., 2025). However, processes of systematic intrusion of its riparian buffer zones have been taken to a higher level by the fast process of urbanization, a lack of institutional capacity to plan spatial issues, poverty, limited housing opportunities and mass displacement due to the Boko Haram insurgency since 2009 (Shettima et al., 2025; Balogun et al., 2020; Nkwocha et al., 2020). These forces have led to a rise in more severe cases of flooding events, with the most recent and worst-case scenario still occurring in September 2024 after the Alau Dam collapse caused at least 37 deaths and displaced more than 400,000 people (International Organization for Migration, 2024; NEMA, 2024), an impact that was further exacerbated by extensive riparian buffer encroachment and reduced channel conveyance along River Ngadda.

Riparian buffer zones (setbacks) have various environmental and hydrological roles, which are important to flood control: (a) storage of temporary floodwater; (b) attenuation of surface runoff; (c) filtration of sediment, and (d) conservation of aquatic life (Graziano et al., 2022; Majumdar and Avishek, 2025). The typical effective buffer widths in the world are 30 to 100 m in accordance with the order of streams, slope, and protection goals (Graziano et al., 2022; Stoffyn-Egli and Duinker, 2013; Sweeney and Newbold, 2014). Buffer width recommendations are generally narrower in African contexts, with South Africa suggesting 32 m in non-perennial rivers, and 100 m in perennial rivers (DWAF, 2005), whereas Ghana suggests 10 to 90 m depending on the order of the streams, the slope, and the danger of pollution (Ministry of Lands and Natural Resources, 2013).

Nigeria has statutory riparian setbacks of between 10 and 60 m across states but there is lack of enforcement. Floods through empirical GIS studies of Abuja, Ilorin, Oyo, Ile-Ife, and Lagos continuously exhibit that buildings located within 30m of river channels are the most vulnerable to floods (Odedare et al., 2017; Adigun et al., 2017; Olajuyigbe et al., 2012; Oriola and Bolaji, 2012). Although the available literature has defined general trends of flood prone areas in Nigerian urban settings, it has not applied a structured model in the quantification of graded breach of riparian buffer at the scale of the individual structure in addition to not having interrogated whether flood exposure along riverine platforms is spatially clustered or dispersed- knowledge gaps that this study intends to fill along the River Ngadda. Further, there is no research study that specifically evaluated the riparian corridor of River Ngadda, even though Maiduguri was affected by catastrophic flooding on a frequent basis. This paper utilizes graduated buffer of 10 m, 20 m, and 30 m to determine the level of encroachment and vulnerability of the river to flood along River Ngadda. This range represents: (1) the minimum statutory setback of 10m by the Nigerian Federal Water Resources Act and the minimum statutory riparian setback of about 10 to 16m in Maiduguri (Borno State Geographic Information System) in forming the inner buffer limit; (2) empirical studies of Nigerian cities showing that most flood damage is within 30m of the channel in wet seasons (Komolafe et al., 2015).

The relationships between fast urbanization, riparian encroachment, and exposure to urban flooding are theorized on the basis of the Human-Environment Interaction Model (Figure 1). This model outlines the role of anthropogenic influences including. population increase, expansion of the informal settlements and poor governance as the triggers of environmental disturbances which included the erosion of the buffer zones and blockage of channels increasing the likelihood of floods. This paper operationalizes these relationships by: (1) measuring the encroachment of buffer zones in terms of the number of buildings in the graduated setback; (2) measuring vulnerability of buildings in terms of distance indices; and (3) analyzing spatial patterns in terms of autocorrelation in order to understand whether encroachment is due to coordinated development or haphazard, opportunistic expansion. As part of urban resilience models, the ability of cities to absorb, adapt, and recuperate following flood shocks is critically determined by the integrity of riparian corridors as natural infrastructure (UN-Habitat, 2020). The current paper states that the governance of floods in Maiduguri can be characterized by a compliance gap, which is promoted in the literature concerning risk governance, despite the existence of statutory setback mechanisms, the institutional means of their enforcement is lacking (Majumdar and Avishek,

ISSN 2278-2540 | DOI: 10.51583/IJLTEMAS | Volume XV, Issue II, February 2026

2025). It is thus necessary to Embed riparian management within the overall urban resilience measures such as community-based monitoring and adapting land-use governance to generate a bridge linkage between this gap and alleviating exposure to buildings to flood risks on the River Ngadda. The study aims to: (1) to quantify the degree of building encroachment within 10m 20m and 30m riparian buffers along River Ngadda; (2) to compute segment-specific Vulnerability Indices that can forecast high-risk areas; (3) to examine the patterns of vulnerability spatial distribution with the aim to inform specific policy interventions.

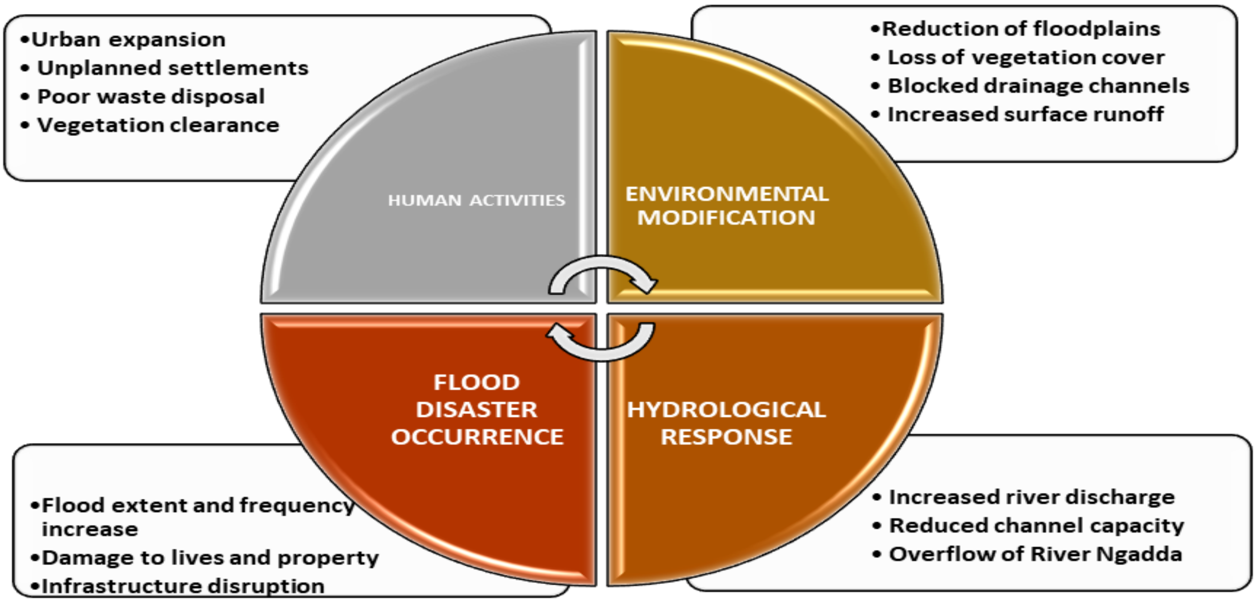

Figure.1 Human–Environment Interaction Model for Flood Risk

Study Area and Methodology

Study Area

Maiduguri is situated between 11°42′00″N and 12°00′00″N, and 12°54′00″E and 13°20′00″E, the area of which is about 648 km2 (Figure. 2). The city is located in the semi-arid Sahelian region of northeastern Nigeria and has unimodal rainfall regime, where the rainy season is usually between June and September and highest in August. During wet years rain can start as early as in April and last until to October. The average annual temperatures are between 30°C and 40°C with temperatures in the dry-season hitting up to 42°C, and Harmattan temperatures can drop down to about 15°C. The major urban drainage system that drains Maiduguri is River Ngadda and its tributary River Ngaddabul (Shettima et al 2025), which comprises the greatest urban drainage system throughout the city. River Ngadda is the river that is significant in stormwater transportation and flood management. This research paper concentrated on River Ngadda, which is the major flood-prone channel in Maiduguri.

River Segmentation

To capture spatial variation on encroachment and flood exposure by the buffer zone, River Ngadda was further broken down into 5 segments (A- E) using physical features especially major bridges (Figures. 2 and 3). The segments was defined in the following ways:

Segment A: Behind Water Treatment Plant (WTP) to Fori Bridge

Segment B: Fori Bridge to Lagos Street Bridge

Segment C: Lagos Street Bridge to Gwange Bridge

Segment D: Gwange Bridge to Custom Bridge

ISSN 2278-2540 | DOI: 10.51583/IJLTEMAS | Volume XV, Issue II, February 2026

Segment E: Custom Bridge to Moromoro Bridge

This segmentation allowed to assess the vulnerability of the river to encroachment by building portions and buffer zones on a segment-by-segment basis.

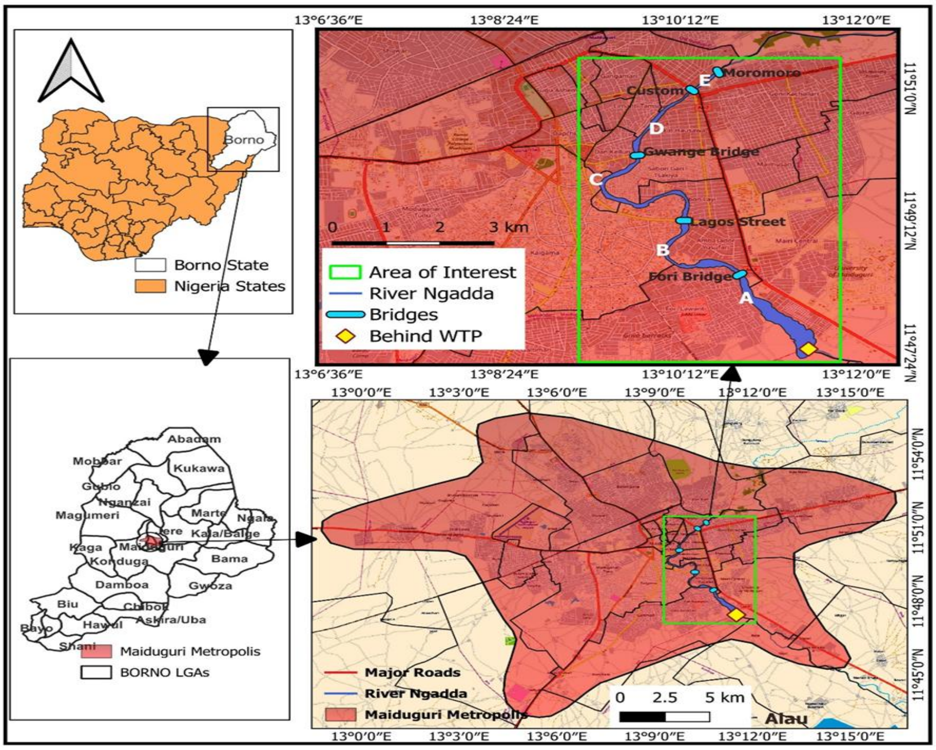

Figure. 2: Study Area Map

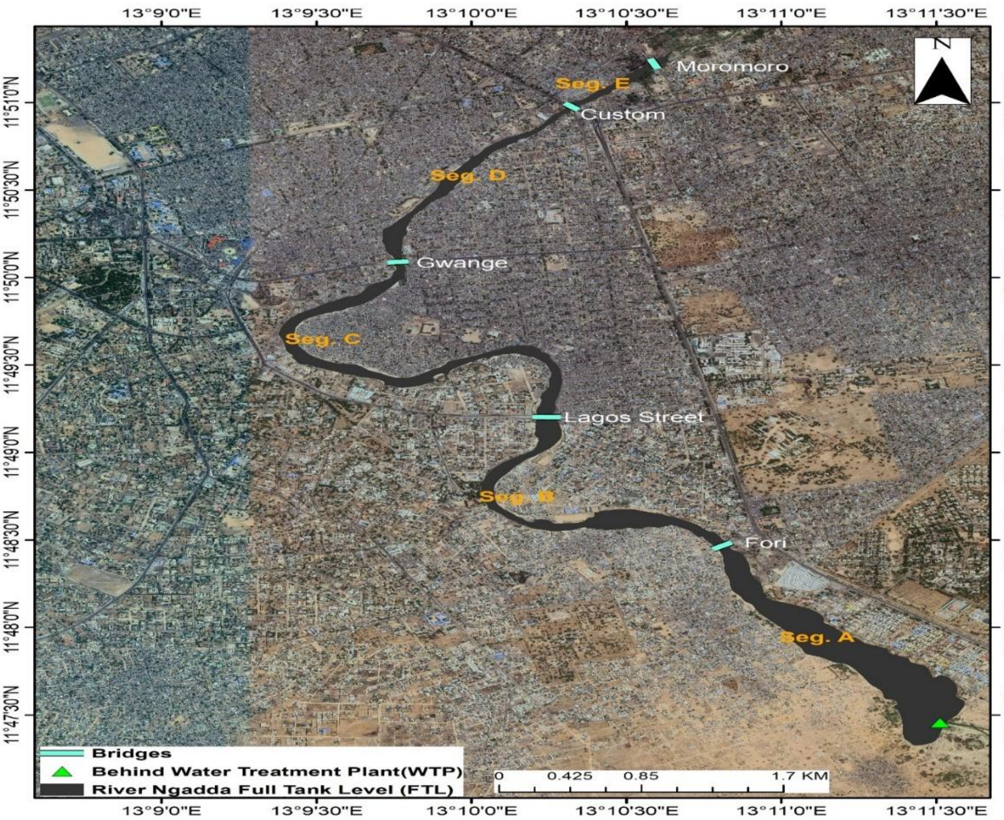

Figure 3: Satellite Imagery of the Study Area

ISSN 2278-2540 | DOI: 10.51583/IJLTEMAS | Volume XV, Issue II, February 2026

Data Sources and Processing

The data of this study was based on the data of two major sources (Table 1). Data on building footprints were acquired by the Microsoft Global Building footprints dataset which offers polygon representations of building outlines, as the result of machine-learning categorization of high-resolution satellite images. High spatial coverage, vector format, and a consistent geometry characterize the dataset, and render it appropriate to the spatial analysis of urban scale. However, past research has demonstrated that these automatically generated datasets can fail to capture emerging trends or informal networks of various cities that are growing at rapid rates (Braun, et al., 2023).

In order to overcome these constraints, the dataset was validated and revised by GeoEye-1 satellite imagery having a spatial resolution of 3.96 cm (Fig. 3). GeoEye imagery has enough spatial resolution to discover discrete buildings, roof profiles and new developments and is suitable to be manually digitized and refine accurateness in data-averse urban settings. Visual comparison of the GeoEye imagery showed that 287 structures had been removed, 143 polygons had been misdigitized, and 89 of the structures were obsolete; the anomalies were later corrected by manually digitizing in ArcGIS 10.8.2. About 17 per cent of the total layer of buildings required modification, mainly in informal settlements which were tightly packed together along Segments C and D. A positional-accuracy test with 50 ground control locations had a root-mean-square error (RMSE) of 1.2m, which is well within acceptable limits of building-scale analysis of flood vulnerability.Figure 4. depicts the Methodological workflow.

Table 1: Summary of Datasets and Data Sources

Dataset	Source	Spatial Resolution	Link
Building Footprints (Initial)	Microsoft Global ML Building Footprints	Vector	https://github.com/microsoft/GlobalMLBuildingFootprints
High-Resolution Satellite Imagery	GeoEye-1	3.96 cm	https://earth.esa.int/eogateway/missions/geoeye-1
Administrative Boundaries	FAO(Global Administrative Unit Layers) Dataset	Vector	http://www.fao.org/geonetwork/srv/en/main.home

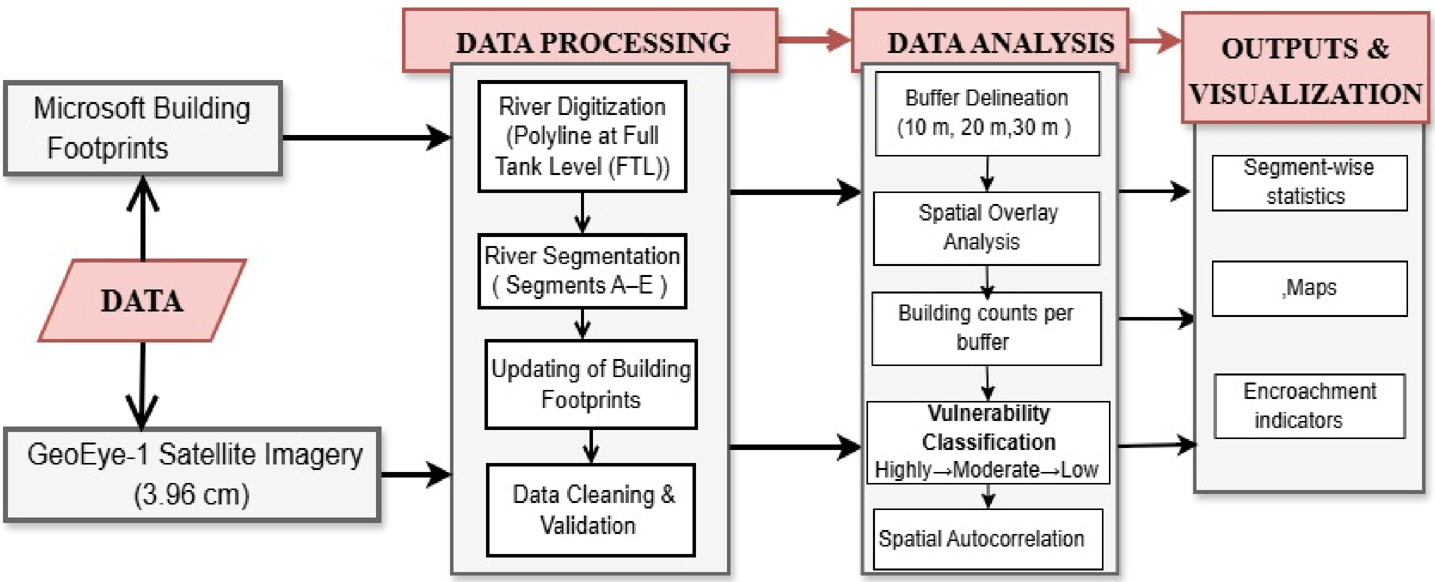

Figure 4. Methodological workflow

ISSN 2278-2540 | DOI: 10.51583/IJLTEMAS | Volume XV, Issue II, February 2026

River Digitization

The high-resolution imagery was used to perform a manual digitization of River Ngadda in ArcGIS 10.8.2. The digitization was performed at Full Tank Level (FTL) of the river, which is the farthest point along the river at high water levels. FTL was determined based on visual analysis of channel morphological indicators such as: (1) vegetation transition zones which indicate the upper limit of regular inundation, (2) alteration in soil moisture pattern that could be observed in the imagery, (3) channel bank profiles and (4) high-water marks and sediment deposits that could be seen. Even though the data of continuous hydrological gauges were not provided, this method is equivalent to the existing knowledge on floodplain delineation in data-sparse settings (Flannery et al., 2017; Wu et al., 2012; Bradbrook et al., 2004). While this visual interpretation method is appropriate for data-scarce contexts, it introduces some uncertainty in precise FTL delineation, particularly in heavily built-up

Data Analysis

Buffer Zone Delineation

In order to determine the amount of encroachment and flood exposure in the buffer zone, three concentric buffer areas (10, 30 ,20 m) were created using the Buffer tool of ArcGIS 10.8.2 based on the digitised riverbank at FTL. The choice of buffer distances was based on the criteria provided in the Introduction which represents the requirements of Borno State Geographic Information System (BOGIS) minimum setback requirements (10-16m), empirical flood thresholds based on Nigerian studies (Odedare et al., 2017; Olajuyigbe et al., 2012) and the hydrological behaviour of River Ngadda during extreme events e.g. the 2024 Alau Dam failure.

Spatial Overlay and Building Counts

Footprints were superimposed on all buffers zones using the Select by Location and Intersect tools of ArcGIS. The total of all buildings intersecting the buffer was calculated using the summary statistics on the field of buildings, the Count function of the Summary Statistics tool was used to count the number of buildings intersecting the buffer distance and river segment as:

Total buildings in 10 m buffer = N_{10}

Total buildings in 20 m buffer = N_{20}

Total buildings in 30 m buffer = N_{30}

Building Vulnerability Classification

The creation of vulnerability to flooding was categorized into three groups based on the distance to the river channel, which was used as a proxy to flood exposure intensity. According to this distance-based method, the intensity of flood hazard decreases over the distance of the river channel, which is based on the results of a variety of studies of urban flood risks (Ghosh, et al., 2023; Islam, et al., 2025). A cumulative subtraction technique ensured mutually exclusive classification across buffer zones, with each building counted once in its closest buffer zone. Exclusive Building Counts were calculated through equations 1-4 and Building density was computed as using question 5.

$$N_{10-\text{exclusive}} = N_{10} \quad (1)$$

$$N_{20-\text{exclusive}} = N_{20} - N_{10} \quad (2)$$

$$N_{30-\text{exclusive}} = N_{30} - N_{20} \quad (3)$$

$$N_{\text{total}} = N_{10-\text{exclusive}} + N_{20-\text{exclusive}} + N_{30-\text{exclusive}} \quad (4)$$

$$Di = \frac{N_i}{A_i} \quad (5)$$

ISSN 2278-2540 | DOI: 10.51583/IJLTEMAS | Volume XV, Issue II, February 2026

Where:

$N_{10-\text{exclusive}}$= Buildings exclusively within 0-10 m buffer

$N_{20-\text{exclusive}}$= Buildings exclusively within 10-20 m zone (within 20 m buffer but outside 10 m buffer)

$N_{30-\text{exclusive}}$= Buildings exclusively within 20-30 m zone (within 30 m buffer but outside 20 m buffer)

D_i = building density for segment i (buildings per square meter, buildings/m²)

N_i = number of buildings within the buffer zone of segment i

A_i = area of the buffer zone for segment i (m²)

The highly vulnerable buildings were all those found within the 10-meter buffer zone ($0 \le d < 10$ m). Moderately vulnerable were the buildings in the range of 10-20 meters ($10 \le d < 20$ m). The buildings falling within the range of 20-30 meters ($20 \le d < 30$ m) were identified as low vulnerability. The proximity classification is not aimed at the actual prediction of flood destruction but simply gives a summary of relative exposure to floods. Even though the vulnerability may be moderated by the ancillary variables like elevation or construction materials, distance to the river remains a robust first-order proxy in urban areas where data are scarce (Komolafe et al., 2015).

The Vulnerability Index (VI) for each segment was calculated using equation 6

$$VVI_s = \frac{(N_{HV}\times3)+(N_{MV}\times2)+(N_{LV}\times1)}{N_{\text{total}}} \quad (6)$$

Where:

VI_s= Vulnerability Index for segment s

N_{HV}= Number of highly vulnerable buildings

N_{MV}= Number of moderately vulnerable buildings

N_{LV}= Number of low vulnerability buildings

N_{total}= Total buildings in all buffer zones for segment

Weight factors: 3 (high), 2 (moderate), 1 (low)

The Vulnerability Index (VI) has a range of 1.0 (corresponding to a situation where all buildings are in a low-vulnerability region) to 3.0 (corresponding to a situation where all buildings are in a high-vulnerability region), and provides a quantitative approximation of how the concentration of flood risk is concentrated in few river segments. The weighting system which has been adopted in this paper, that is, the ratio 3:2:1, is heuristic in nature and assumes the intensity of flood-hazards to decrease linearly with the spatial distance. Only slight differences in the relative ranking of the segments were obtained after a sensitivity analysis using different weighting (4:2:1) and weighting combinations (3:1.5:1) and this indicates that the outcome obtained is robust to a moderate variation in the weighting parameters.

Spatial Autocorrelation Analysis

To examine the spatial pattern of flood vulnerability along River Ngadda, spatial autocorrelation analysis determined whether vulnerable buildings are randomly distributed or spatially dependent. Building footprints were converted to centroid points with vulnerability scores depending on the distance to buffers (3, 2 and 1,

ISSN 2278-2540 | DOI: 10.51583/IJLTEMAS | Volume XV, Issue II, February 2026

respectively: 0-10m, 10-20m and 20-30m). The performance of Spatial Autocorrelation (Global Moran I) was done in ArcGIS 10.8.2 with the help of an inverse-distance spatial weights matrix. The inverse-distance weighting scheme was chosen due to the fact that it is suitable in terms of the hypothesis according to which spatially close buildings are more likely to have similar levels of vulnerability since they have similar environmental background and development trends. A threshold of conceptualization distance of 100m was used, as it was proposed by the average size of informal settlements localities in Maiduguri. The Moran's I values ranges between +1 and -1, which implies that the spatial dispersion, randomness, or concentration of the levels of vulnerability is present, which in turn enhances the spatial flood risk assessment.

RESULTS AND DISCUSSION

Spatial Distribution of Riparian Buffer Encroachment Along River Ngadda

Spatial analysis revealed that there is massive encroachment into the riparian buffer zones in all the five segments of the river (Figures 5-10, Table 2). Across all segments, 716 building were found within 10m buffer, 1,904 building within 20m buffer and 3,065 building within 30m buffer. Segment C exhibited the highest encroachment at any distance of the buffers, with 330 buildings at 10m distance, 881 at 20m distance and 1,433 at 30m distance. Segment B and D had heavy encroachment as well with Segment B having 132, 342, and 524 structures in 10m, 20m, and 30m buffers, respectively and Segment D having 151, 413, 653 structures respectively. Segment A and E were in the lower encroachment levels with the 29 and 74 buildings respectively in their 10m buffer environments but the fact that there are 143 and 312 buildings in their 30m buffer environment is testimony to continued development pressure in these marginal areas. Normalized to the buffer area, the patterns of building density indicated that there was spatial variation between the segments (Table 2). Segment E had the greatest density (0.001241 buildings/m^2) in the 10m buffer, then Segment C (0.000879 buildings/m^2) and Segment D (0.000835 buildings/m^2). This density trend was also observed through the 20m and 30m buffers, as Segments E, C and D all exhibited the highest proportion of structures per square meter of available riparian corridor area.

Table 2: Spatial Distribution Segment-wise Buffer Zone Area, Building Counts, and Density across 10m, 20m, and 30m Buffer Distances

Buffer 10m	**Segment**	**Buffer Area (m²)**	**Building Count**	**Density (buildings/m²)**	**Rank by Density**
	A	692,287.00	29	0.00004189	5
	B	314,588.00	132	0.00042	4
	C	375,472.00	330	0.000879	2
	D	180,921.00	151	0.000835	3
	E	59,632.80	74	0.001241	1
	Total	1,622,900.80	716	0.000441	-
Buffer 20m	**Segment**	**Buffer Area (m²)**	**Building Count**	**Density (buildings/m²)**	**Rank by Density**
	A	748,130.00	47	0.00006282	5
	B	368,941.00	210	0.000569	4
	C	449,776.00	551	0.001225	2
	D	222,391.00	262	0.001178	3
	E	76,082.00	118	0.001551	1
	Total	1,865,320.00	1,188	0.000637	-
Buffer 30m	**Segment**	**Buffer Area (m²)**	**Building Count**	**Density (buildings/m²)**	**Rank by Density**

ISSN 2278-2540 | DOI: 10.51583/IJLTEMAS | Volume XV, Issue II, February 2026

	A	804,184.00	143	0.000178	5
	B	423,043.00	182	0.00043	4
	C	523,958.00	552	0.001054	2
	D	263,786.00	240	0.00091	3
	E	92,825.90	120	0.001293	1
	Total	2,107,796.90	1,237	0.000587	-

Note: Density is reported as buildings per square meter (buildings/m²) for comparability across segments with differing buffer areas.

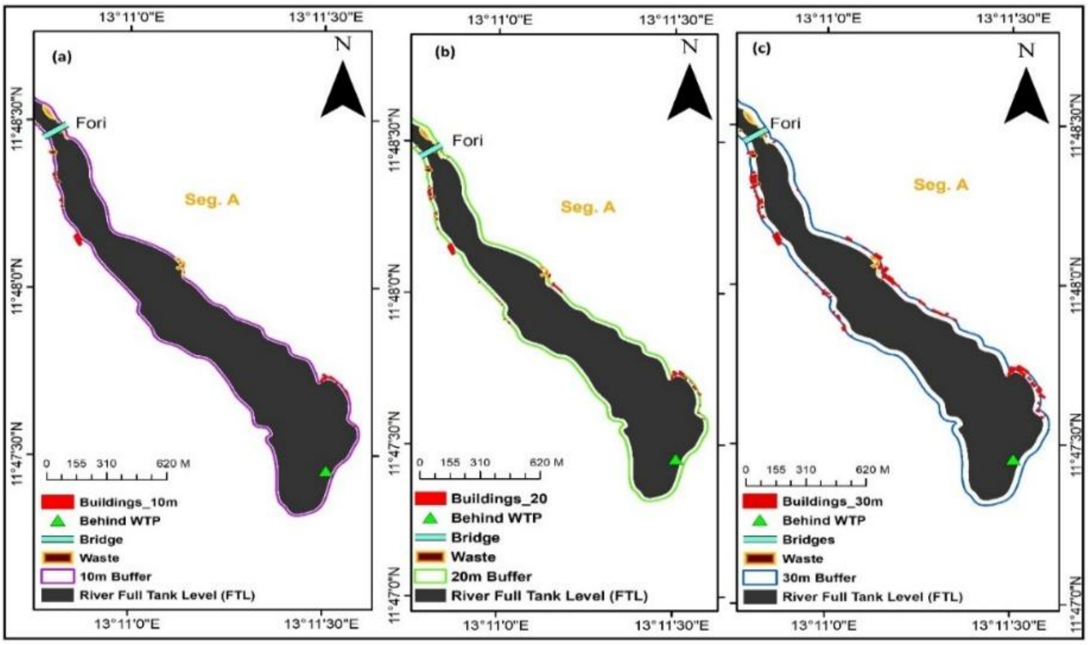

Figure. 5. Buildings encroachment within (a) 10 m, (b) 20 m, and (c) 30 m river buffer zones along Segment A

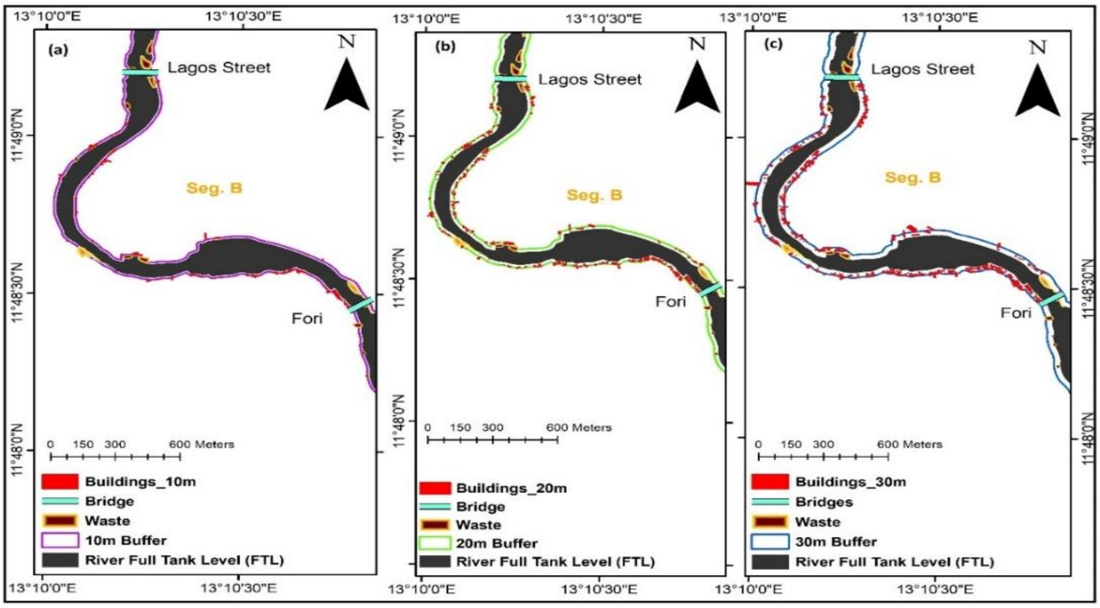

Figure. 6. Buildings encroachment within (a) 10 m, (b) 20 m, and (c) 30 m river buffer zones along Segment B

ISSN 2278-2540 | DOI: 10.51583/IJLTEMAS | Volume XV, Issue II, February 2026

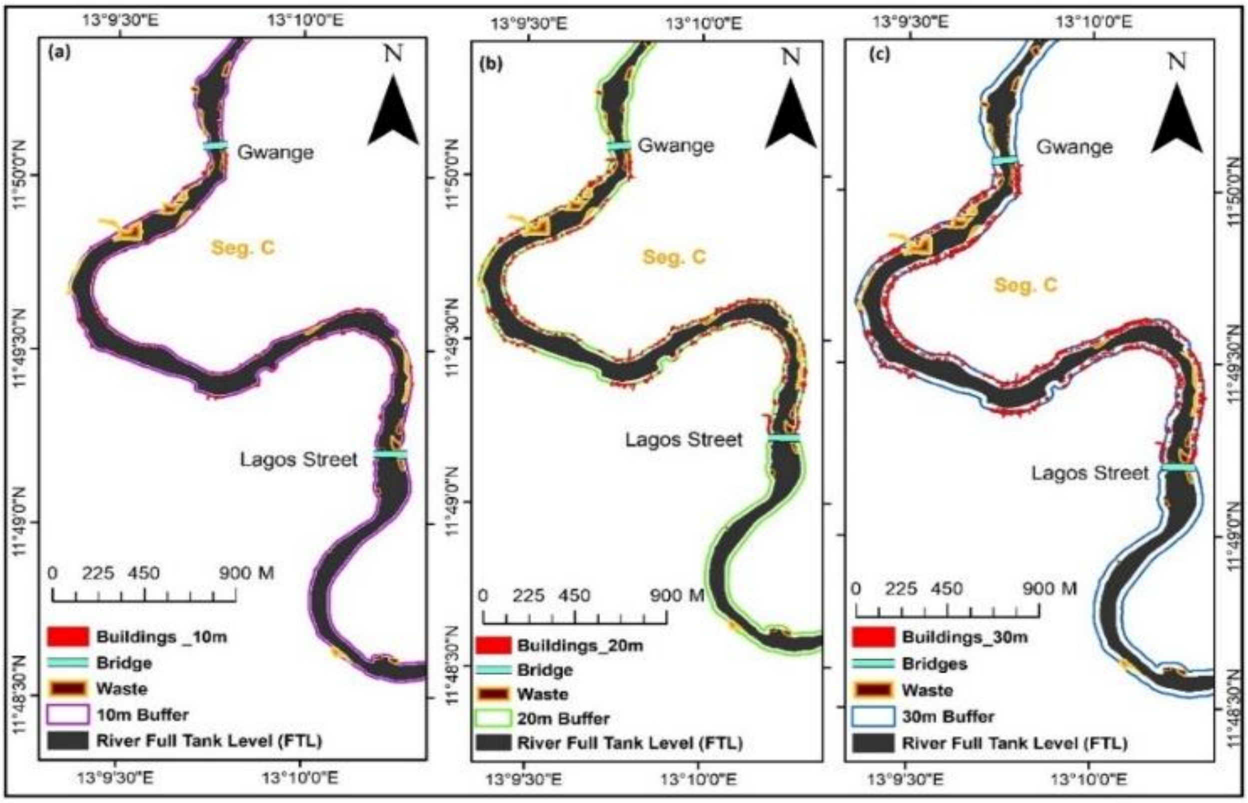

Figure. 7. Buildings encroachment within (a) 10 m, (b) 20 m, and (c) 30 m river buffer zones along Segment C

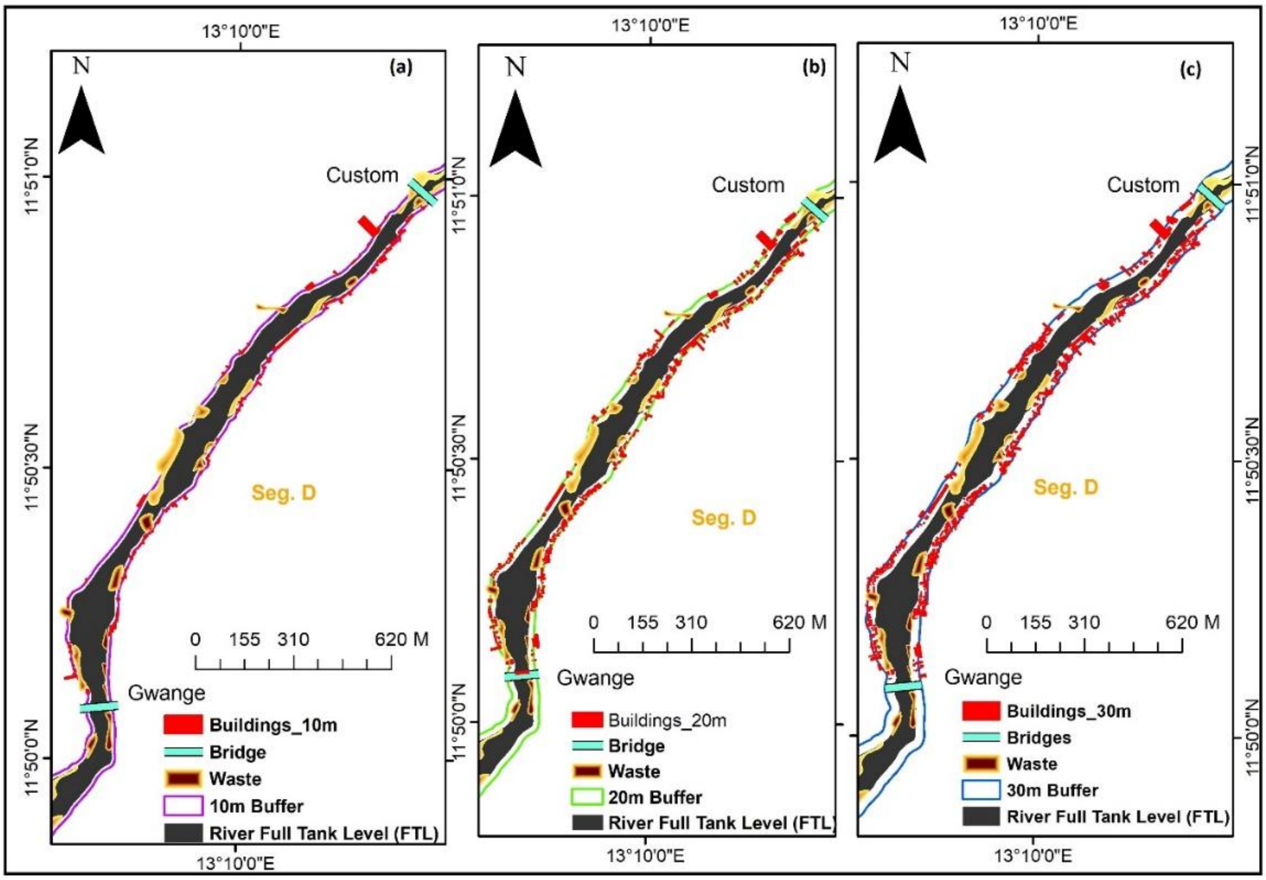

Figure 8. Buildings encroachment within (a) 10 m, (b) 20 m, and (c) 30 m river buffer zones along Segment D

ISSN 2278-2540 | DOI: 10.51583/IJLTEMAS | Volume XV, Issue II, February 2026

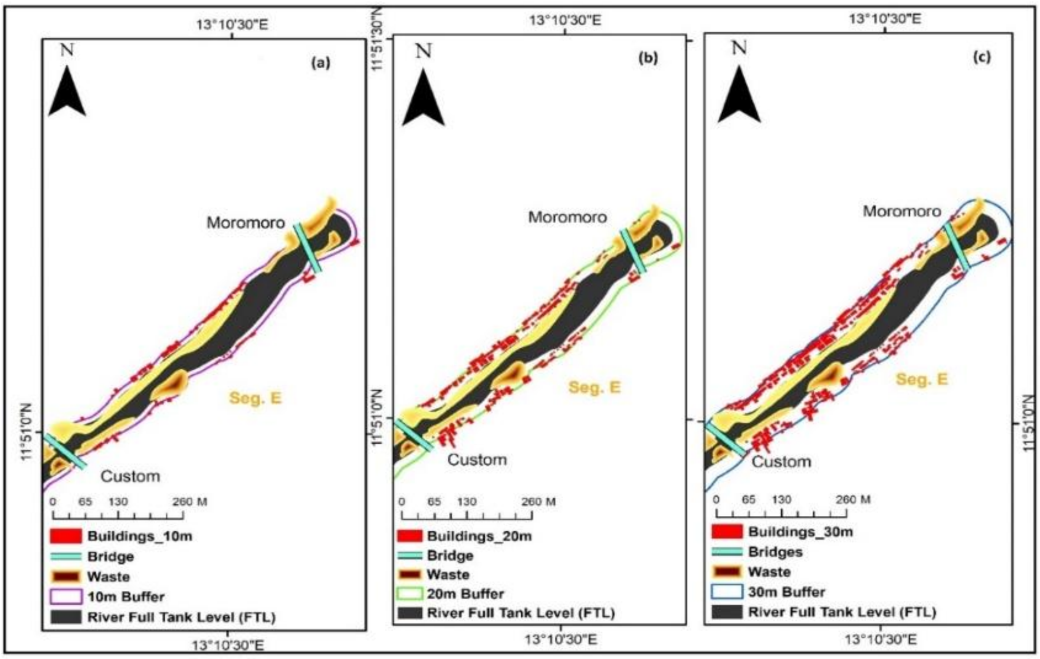

Figure 9. Buildings encroachment within (a) 10 m, (b) 20 m, and (c) 30 m river buffer zones along Segment E

Building Vulnerability Classification and Segment Vulnerability Index

Building vulnerability classification demonstrated that there was a high level of spatial variation in the concentration of flood risk across River Ngadda (Table 3). Across all segments, 716 buildings were classified as highly vulnerable (0-10m), 1,188 as moderately vulnerable (10-20m), and 1,161 as low vulnerability (20-30m), with a calculated VI value ranging between 1.73 and 1.90 and an average of 1.85. Segment B was the most vulnerable (VI = 1.90), then there were Segments D (1.86), E (1.85), C (1.84) and A (1.73).

The distribution of buildings in terms of vulnerability (716:1,188:1,161) show that there are fairly balanced encroachment quantities throughout the entire 30m wide corridor instead of a concentration in the safer outer zones.

Table 3: Building Vulnerability Classification and Segment Vulnerability Index

Segment	Highly Vulnerable (0-10m)	Moderately Vulnerable (10-20m)	Low Vulnerable (20-30m)	Total Buildings	Vulnerability Index (VI)
A	29	47	67	143	1.73
B	132	210	182	524	1.9
C	330	551	552	1,433	1.84
D	151	262	240	653	1.86
E	74	118	120	312	1.85
Total	716	1,188	1,161	3,065	1.85

Note: *Vulnerability Index (VI) calculated using Equation 6* $VI_s = \frac{(N_{HV}\times 3)+(N_{MV}\times 2)+(N_{LV}\times 1)}{N_{total}}$*, where VI ranges from 1.0 (lowest risk) to 3.0 (highest risk).*

Spatial Autocorrelation Analysis

Segment-wise Global Moran's I analysis revealed predominantly negative spatial autocorrelation across most segments (Table 4, Figures 10a-e), indicating a dispersed and not clustered pattern of vulnerability. Segment A

INTERNATIONAL JOURNAL OF LATEST TECHNOLOGY IN ENGINEERING, MANAGEMENT & APPLIED SCIENCE (IJLTEMAS)

ISSN 2278-2540 | DOI: 10.51583/IJLTEMAS | Volume XV, Issue II, February 2026

had low dispersion (Moran I = -0.0706, Z -score = -1.553, p = 0.12) which was not statistically significant, implying almost a random distribution of vulnerability. Segments B through E all demonstrated statistically significant negative autocorrelation. Segment D had the most significant dispersion (Moran I = -0.1524, Z-score = -12.110, p < 0.001), then followed by Segment B (Moran I = -0.1017, Z-score = -11.922, p < 0.001), Segment C (Moran I = -0.0778, Z-score = -7.850, p < 0.001), and then Segment E (Moran's I = -0.0594, Z-score = -2.648, p = 0.008).

Table 4: Segment-wise Spatial Autocorrelation (Moran's I) of Building Flood Vulnerability

River Segments	Moran's I	Expected I	Variance	Z-score	p-value	Spatial Pattern	Significance
A	-0.0706	-0.0040	0.00184	-1.553	0.12	Weak dispersion	Not significant
B	-0.1017	-0.0008	0.00007	-11.922	<0.001	Strong dispersion	Significant
C	-0.0778	-0.0004	0.0001	-7.850	<0.001	Moderate dispersion	Significant
D	-0.1524	-0.0007	0.00016	-12.110	<0.001	Very strong dispersion	Significant
E	-0.0594	-0.0017	0.00047	-2.648	0.008	Moderate dispersion	Significant

Note: Expected I values differ across segments because Moran's I was computed separately for each segment using segment-specific feature counts (n), where Expected I = −1/(n−1).

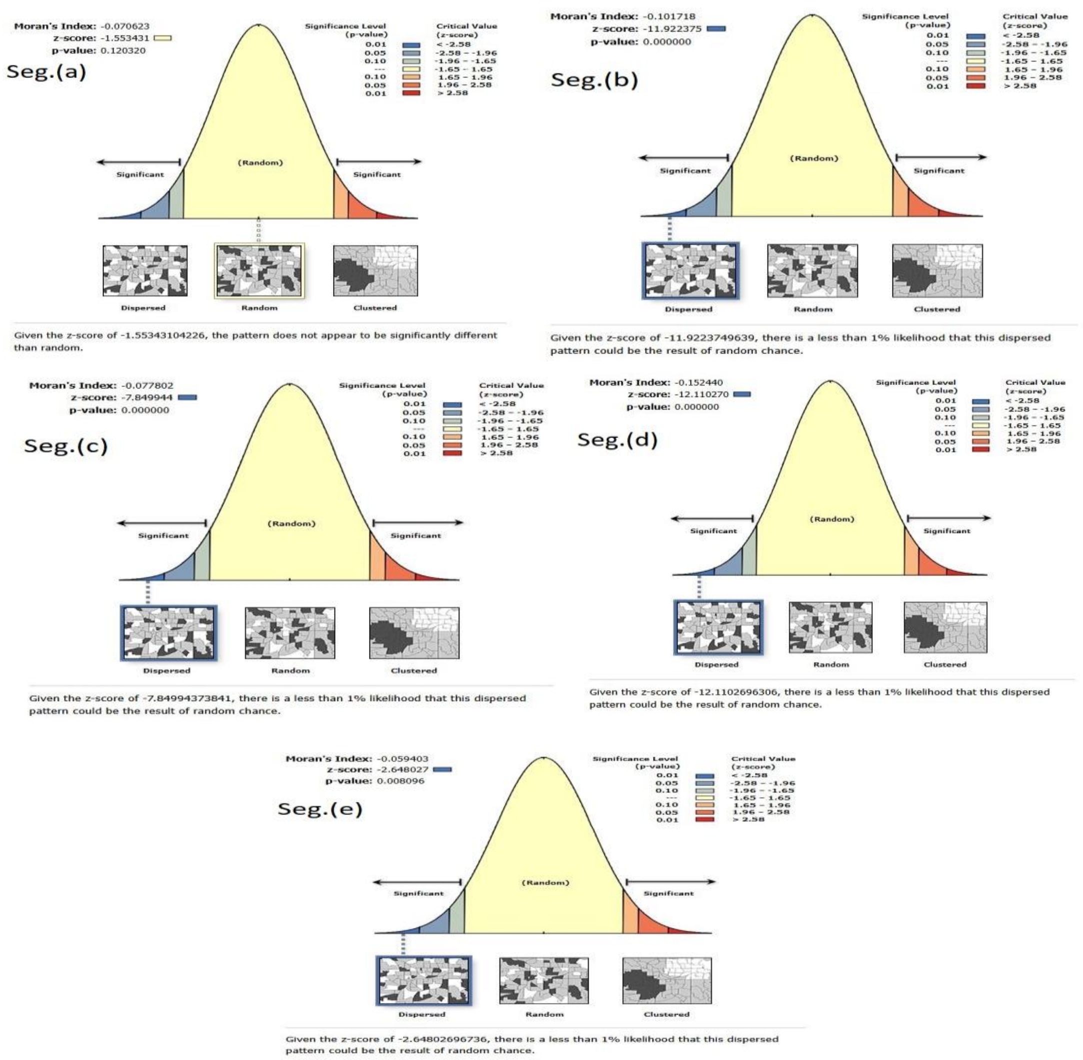

Figure. 10: Segment-wise Spatial Autocorrelation (Moran I) Report: Segments (a)-(e)

ISSN 2278-2540 | DOI: 10.51583/IJLTEMAS | Volume XV, Issue II, February 2026

DISCUSSION

The high extent of encroachment recorded along River Ngadda is an indication of massive breach of riparian setback laws, which are in accord with the findings recorded in other towns within Nigeria (Bakare et al., 2019; Odedare et al., 2017; Olajuyigbe et al., 2012). High rates of urbanization with a low level of enforcement have promoted the growth of building into the riparian land, which is probable to increase flood risk. The proximity to the channel increases the likelihood of the structure to be impacted, including inundation, high-velocity flows, and bank erosion, and the study proved that close buildings sustain disproportionately greater damages due to permanent causes (Mansouri et al., 2025; Choorapulakkal et al., 2024; Malgwi et al., 2021). This continuous rise in the number of buildings as the buffer distances increase argues in favor of continual erosion that reduces the ability of the river to deal with its floods in a natural way.

The average of the values of Vulnerability Index (VI) (1.73-1.90; mean 1.85) shows moderate-high exposure along the corridor, and the distribution of the buildings is even within the 30 m buffer as opposed to safer exterior areas-a trend in other encroached systems (Manna et al., 2025; Komolafe et al., 2015). Comparisons of VI-density indicate complementarities. The high VI (1.90) of segment B even though it is moderately dense is a bank concentration indicator. Segment E has a high density, which provides lower VI (1.85) with even distribution. Both are compounding risks of segment C. The VI therefore represents a relative exposure measure rather than a deterministic predictor, as it excludes elevation, construction materials, drainage capacity, and flood depth — variables that future multi-parameter frameworks should incorporate.

Field observations also found out that patterns of waste and drainage obstruction also gives more context to vulnerability on top of distance and density measures. Segments C, D, and E showed a high level of solid waste dumping on the channel (Figures 5-9), which is reflected in their higher VI values (1.84-1.86) and can assert that the increased risk of flooding in these segments can be multiplied by the decreased capacity of the channel (Komolafe et al., 2015; Mokuolu et al., 2022; Echendu, 2023). Conversely, Segment A, which had comparatively more buildings near the channel, had comparatively little waste and the lowest VI (1.73) which implies that channel maintenance conditions might cause distance-based exposure to moderate.

The essentially negative Moran’s I values (considerable variation in Segments B-E) are not in line with the normal patterns of clustering observed in flood-prone urban rivers and reflects fragmented, and not concentrated, vulnerability. This dispersion could be explained in a number of ways. To start with, uncoordinated informal urbanization with individualized land use, housing shortage, and lax enforcement of these conditions can be the baseline of dispersion, which fits the dynamics of post-displacement in Maiduguri (Nkwocha et al., 2020). Second, variable land tenure regimes can result in unequal enforcement topography leading to dispersed and not clustered encroachment. Third, historic infrastructure such as bridges might have impacted settlement patterns in unequal measures, forming scattered and not continuous vulnerable areas. Fourth, topographic differences in floodplain can form areas of high or low land that can influence a location decision without regard to the distance of the channel. Although the former seems to be the most appropriate in the context of local conditions, the existing data cannot make a certain distinction between these options. The insignificant outcome in Segment A could be due to reduced development pressure in the urban fringe close to the infrastructure facilities.

From an enforcement standpoint, the scattered nature of the encroachment as indicated by negative Moran's I values poses a very different challenge than the clustered violations. Clustered encroachment enables the authorities to act upon adjacent areas in concert, whereas dispersed encroachment, as in this case, requires them to intervene at parcel scales, not at area scales. This has practical consequences on resource allocation - enforcement agencies in Maiduguri should focus on mobile and responsive systems and not fixed-zone policing, and community land committees might be granted the power to report isolated violations in real-time. This observation further supports the importance of segment specific strategies presented in the Policy Implications section, as homogenous implementation mechanism would ill-fit the spatial fragmentation of encroachment measures recorded on River Ngadda.

Segments B, C, and D all record high VI values (1.84–1.90) but differ markedly in the character and mechanisms of their vulnerability. The area with the most absolute buildings (1,433 within 30m including 330 in the high-risk 0-10m area), is segment C, traversing the commercial core of Maiduguri, although it is densely developed with residential and commercial activities, the distribution in the buffer zones is relatively balanced (VI = 1.84). Conversely, Segment B, which contains fewer total buildings (524 within 30m) has the highest VI (1.90) because, although only 25.2% of its total buildings fall within the 0–10m zone, this represents the highest proportional concentration of any segment at that distance (62.4% relative share; Table 3). Segment D has a high number of buildings (653 in 30m) as well as the most intense spatial dispersion (Moran's I = -0.1524), indicating a qualitatively different settlement pattern of mixed older established settlements and new informal development around Custom Bridge. The differences between central segments reflect that central vulnerability to segments C, B and D is associated with density-related pressure, proximity-related exposure, and fragmented incremental growth, respectively. Segments A and E, which are peripheral, have alarming expansion rates of 143 and 312 buildings in the 30m buffers. The most vulnerable areas are always the central areas with the greatest density of bridges, the closest to the market, and the longest histories of settlement, meaning that the flood risk is a phenomenon of complex interactions among developmental processes, land economies, and infrastructure location instead of the even distribution.

Limitations

A number of constraints should be mentioned. Footprint data that is built up might still have residual errors notwithstanding the attempt to validate it. Although field observations provided qualitative evaluation of waste deposition and drainage states in various segments, no systematic quantitative measures of blockage density, blockage position, or infrastructure state were provided in this study, which did not allow conducting a more rigorous sensitivity analysis of these variables. The temporal differences between floods (2012, 2018, 2024) and imagery (2023-2024) hinder direct effects of the past to the present. FTL interpretation creates subjectivity in vegetated reaches or modified reaches. The VI weighting scheme presupposes proportional reduction of the hazard at a distance which is not necessarily uniform. This is because sensitivity of Moran's I to spatial parameters tends to indicate that other specifications could obtain different variations. Fundamentally, most essentially, vulnerability estimates show likely relative exposure and not essentially quantified threat because of lack of hydraulic modeling. The proposed research method needs to be combined with hydrodynamic modeling, Digital Elevation Models, multi-temporal analysis, and socio-economic indicators in the future to enhance evidence and allow quantifying the risk.

Policy Implications

The results indicate that there is an immediate need to have spatially focused management instead of standard policies. Segments B, C and D are highly vulnerable and they need gradual relocation or retrofitting, the setback must be strictly implemented and the waste management courses, and only community-based monitoring can be used to supplement the official supervision. The preventive enforcement of the A and E peripheral segments is necessary prior to the reestablishment of the conditions in the central. The local attributes need to be analyzed within the framework of segment-specific strategies: waste management of the market-area and settlement-upgrading in Segment C, alternative water access to commercial activity in the Segment B, tenure-based differentiation in Segment D. It is necessary to be implemented through institutional strengthening such as land tenure clarification, inter-agency coordination, development of capacity to enforce and participate in planning in a particular segment.

CONCLUSION

This paper shows the riparian invasion in the Ngadda River is pronounced, with 3,065 structures located within the 30m riparian zone, of which 716 were in the highest-risk 0–10m buffer, 1,188 in the 10–20m buffer, and 1,161 in the 20–30m buffer, with moderate-to-high Vulnerability Indices ranging from 1.73 to 1.90, indicating widespread and graded setback violations. The distribution of these encroachment and vulnerability patterns is mainly centralized within section B, C, and D of the central segments with scattered distribution pattern as indicated by a negative value of Moran; I (see Table 4). Although distance and density-based measurements are useful in giving complementary data on spatial information, they are made indeterminate by uncertainties on hydraulic modelling forecasts. Based on this, urban resilience in Maiduguri is proposed to be strengthened by conducting urban strategic interventions, including staged relocation and implementation in segments B to D, preventive interventions in segments A and E, systematic waste clearing, as well as institutional reforms.

REFERENCE

1. Adigun, I. A., Ibe, P. O., & Akolo, F. O. (2017). Appraisal of Abuja master plan using GIS: A case study of Abuja Phase I, Federal Capital Territory, Nigeria. World Scientific News, 77(2), 144–162.
2. Amusa, I. A., Ibe, P. O., & Akolo, F. O. (2017). Appraisal of Abuja master plan using GIS: A case study of Abuja Phase I, Federal Capital Territory, Abuja, Nigeria. World Scientific News, 77(2), 144–162.
3. Bakare, G. O., Omosulu, S. B., & Famutimi, J. T. (2019). Geo-mapping of areas vulnerable to Ala-River Basin flood disaster risk in Akure, Ondo State, Nigeria. Preprints. https://doi.org/10.20944/preprints201911.0184.v1
4. Bradbrook, K. F., Lane, S. N., Waller, S. G., & Bates, P. D. (2004). Two dimensional diffusion wave modelling of flood inundation using a simplified channel representation. *International Journal of River Basin Management*, *2*(3), 211–223. https://doi.org/10.1080/15715124.2004.9635233
5. Braun, A., Warth, G., Bachofer, F., Schultz, M., & Hochschild, V. (2023). Mapping Urban Structure Types Based on Remote Sensing Data—A Universal and Adaptable Framework for Spatial Analyses of Cities. Land, 12(10), 1885. https://doi.org/10.3390/land12101885
6. Choorapulakkal, A. A., Madandola, M. G., Al-Kandari, A., Furlan, R., Bayram, G., & Mohamed, H. A. A. (2024). The Resilience of the Built Environment to Flooding: The Case of Alappuzha District in the South Indian State of Kerala. *Sustainability*, *16*(12), 5142. https://doi.org/10.3390/su16125142
7. DWAF (Department of Water Affairs and Forestry, South Africa). (2005). A practical field procedure for identification and delineation of wetlands and riparian areas. Department of Water Affairs and Forestry, Pretoria, South Africa. https://www.dws.gov.za/Documents/Legislature/nw_act/NWA.pdf
8. Echendu, A. J. (2023). Flooding and Waste Disposal Practices of Urban Residents in Nigeria. GeoHazards, 4(4), 350-366. https://doi.org/10.3390/geohazards4040020
9. FGN (Federal Government of Nigeria). (1993). Water Resources Act, Cap W2, Laws of the Federation of Nigeria. Federal Ministry of Water Resources, Abuja, Nigeria
10. Fischer, R. A., & Fischenich, J. C. (2000). *Design recommendations for riparian corridors and vegetated buffer strips* (No. ERDCTNEMRRPSR24). https://apps.dtic.mil/sti/pdfs/ADA378426.pdf
11. Flannery, J., Stubblefield, A., Fiori, R., & Shea, C. (2017). Observations of channel change from constructed wood jams on a forested gravel-bed stream. Transactions of the American Fisheries Society, 146(1), 181-193.
12. Ghosh, A., Chatterjee, U., Pal, S. C., Towfiqul Islam, A. R. Md., Alam, E., & Islam, M. K. (2023). Flood hazard mapping using GIS-based statistical model in vulnerable riparian regions of sub-tropical environment. Geocarto International, 38(1). https://doi.org/10.1080/10106049.2023.2285355
13. Balogun, A. D., Salleh, M. A. Bin, & Ahmad, A. A. (2020). The Effects of Boko Haram Insurgency on The Internally Displaced Children in Nigeria. International Journal of Academic Research in Business and Social Sciences, 10(2), 795–822. http://dx.doi.org/10.6007/IJARBSS/v10-i2/7010
14. Graziano, M. P., Deguire, A. K., & Surasinghe, T. D. (2022). Riparian Buffers as a Critical Landscape Feature: Insights for Riverscape Conservation and Policy Renovations. *Diversity*, *14*(3), 172. https://doi.org/10.3390/d14030172
15. Güneralp, B., Lwasa, S., Masundire, H., Parnell, S., & Seto, K. C. (2017). Urbanization in Africa: challenges and opportunities for conservation. *Environmental research letters*, *13*(1), 015002. **DOI** 10.1088/1748-9326/aa94fe
16. International Organization for Migration. (2024). Nigeria flood situation report — Borno State (13 September 2024) (Update 1). Displacement Tracking Matrix (DTM). https://nigeria.iom.int/sites/g/files/tmzbdl1506/files/documents/reports/Borno_Flood_Situation_Report_13_September_2024_final_0.pdf**

ISSN 2278-2540 | DOI: 10.51583/IJLTEMAS | Volume XV, Issue II, February 2026

17. Islam, T., Zeleke, E. B., Afroz, M., & Melesse, A. M. (2025). A Systematic Review of Urban Flood Susceptibility Mapping: Remote Sensing, Machine Learning, and Other Modeling Approaches. *Remote Sensing*, *17*(3), 524. https://doi.org/10.3390/rs17030524
18. Komolafe, A. A., Adegboyega, S. A. & Akinluyi, F. O. (2015). A Review of Flood Risk Analysis in Nigeria. American Journal of Environmental Sciences, 11(3), 157-166. https://doi.org/10.3844/ajessp.2015.157.166
19. Majumdar, A. & Avishek, K. (2025). Mitigating riparian buffer zone degradation through policy interventions and learnings from best practices. Discov Environ 3, 84 https://doi.org/10.1007/s44274-025-00288-6
20. Malgwi, M. B., Schlögl, M., & Keiler, M. (2021). Expert-based versus data-driven flood damage models: A comparative evaluation for data-scarce regions. International Journal of Disaster Risk Reduction, 57, 102148. https://doi.org/10.1016/j.ijdrr.2021.102148
21. Manandhar, B., Cui, S., Wang, L., & Shrestha, S. (2023). Urban Flood Hazard Assessment and Management Practices in South Asia: A Review. *Land*, *12*(3), 627. https://doi.org/10.3390/land12030627
22. Manna, H., Das, M., Pramanik, M., Sarkar, S., Mahato, S., Talukdar, S. & Zhran, M. (2025). Ensemble intelligence for urban resilience: flood susceptibility modeling in Mumbai using advanced machine learning. *Geomatics, Natural Hazards and Risk*, *16*(1) 2588718. https://doi.org/10.1080/19475705.2025.2588718
23. Mansouri, S., Noroozinejad Farsangi, E., Siahpolo, N., Moghadam, A. S., Pour, A. K., & Noori, M. (2025). Effects of River Shapes on Structural Damages to Buildings in Flood-Prone Regions. Journal of Structural Design and Construction Practice, 30(3), 05025005. https://doi.org/10.1061/JSDCCC.SCENG-1717
24. Ministry of Lands and Natural Resources. (2013). Riparian Buffer Zone Policy for Managing Freshwater Bodies in Ghana. Government of Ghana. https://faolex.fao.org/docs/pdf/gha149365.pdf
25. Mokuolu, O. A., Odunaike, A. K., Iji, J. O., & Aremu, A. S. (2022). Assessing the effects of solid wastes on urban flooding: A case study of Isale Koko. LAUTECH Journal of Civil and Environmental Studies, 9(1), 22–30. https://doi.org/10.36108/laujoces/2202.90.0130
26. NEMA (National Emergency Management Agency). (2024). Flood situation report: Borno State, September 2024. National Emergency Management Agency, Abuja, Nigeria.
27. Nkwocha, K. F., Iheukwumere, S. O., Shettima, M. K., & Audu, A. (2020). *An autopsy of housing challenges in urban Maiduguri*. Open Access Journal of Waste Management & Xenobiotics, 3(4).1-7 https://doi.org/10.23880/oajwx-16000149
28. Nkwunonwo, U. C., Whitworth, M., & Baily, B.:(2016) Review article: A review and critical analysis of the efforts towards urban flood risk management in the Lagos region of Nigeria, Nat. Hazards Earth Syst. Sci., 16 (2) 349–369, https://doi.org/10.5194/nhess-16-349-2016
29. Obroh, O. G., & Sambo, G. (2022). Flood vulnerability mapping of River Ngadda using geospatial and remote sensing techniques in Maiduguri Metropolis, Borno State. Journal of Global Ecology and Environment, 14(4), 44–58. https://doi.org/10.56557/JOGEE/2022/v14i47453
30. Odedare, K. O., Amusa, I. A., Aweda, T. O., & Gbiri, I. A. (2017). Vulnerability assessment of structures along river channels in Oyo metropolis, Nigeria. World Scientific News, 83, 130–149.
31. Olajuyigbe, A. E., Rotowa, O. O., & Durojaye, E. (2012). An assessment of flood hazard in Nigeria: The case of Mile 12, Lagos. Mediterranean Journal of Social Sciences, 3(2), 367–375. https://doi.org/10.5901/mjss.2012.v3n2.367
32. Oriola, E., & Bolaji, S. (2012). Urban flood risk information on a river catchment in a part of Ilorin Metropolis, Kwara State, Nigeria. Information and Knowledge Management, 2(8), 70–83.
33. Sanyaolu, B. O., Ibrahim, U. A., & Alkali, A. N. (2025). Rainfall and Streamflow Dynamics in the Borno Region of the Lake Chad Basin: A Hydrological Assessment. Arid Zone Journal Of Engineering, Technology and Environment, 21(2), 491-498. Retrieved from https://azojete.com.ng/index.php/azojete/article/view/1070
34. Shettima, M., Hasnat, M., Sambo, G. H., Bukar, A. G., Boyoma, A. M., & Mohammed, M. A. (2025). Spatio-Temporal Dynamics and Forecasting of Urban Land Use and Land Cover Change in Maiduguri Using Google Earth Engine and Machine Learning. Arid Zone Journal of Engineering, Technology and Environment, 21,(3) 783-793. https://www.azojete.com.ng/index.php/azojete/article/view/1121

ISSN 2278-2540 | DOI: 10.51583/IJLTEMAS | Volume XV, Issue II, February 2026

35. Stoffyn-Egli, P., & Duinker, P. N. (2013). An ecological approach to riparian-buffer definition, and implications for timber harvests in Nova Scotia, Canada. Journal of sustainable development, 6(12), 111.
36. Sweeney, B. W., & Newbold, J. D. (2014). Streamside Forest Buffer Width Needed to Protect Stream Water Quality, Habitat, and Organisms: A Literature Review†. Journal of The American Water Resources Association, 50(3), 560–584. https://doi.org/10.1111/JAWR.12203
37. Uba, M. I. (2024). Assessing natural disaster and sustainable infrastructure development: A case study of flood resilience and mitigation strategies in Maiduguri, Nigeria. International Journal of Advances in Engineering and Management, 6(10), 244–249. https://doi.org/10.35629/5252-0610244249
38. Umar, N., & Gray, A. (2023). Flooding in Nigeria: a review of its occurrence and impacts and approaches to modelling flood data. *International Journal of Environmental Studies*, *80*(3), 540–561. https://doi.org/10.1080/00207233.2022.2081471
39. UN-Habitat. (2020). *World Cities Report 2020: The value of sustainable urbanization*. United Nations Human Settlements Programme, Nairobi, Kenya. https://unhabitat.org/World%20Cities%20Report%202020
40. USEPA (United States Environmental Protection Agency). (2005). National management measures to control nonpoint source pollution from urban areas. EPA-841-B-05-004. Office of Water, Washington, DC.
41. Wu, H., Adler, R. F., Hong, Y., Tian, Y., & Policelli, F. (2012). Evaluation of Global Flood Detection Using Satellite-Based Rainfall and a Hydrologic Model. Journal of Hydrometeorology, 13(4), 1268-1284. https://doi.org/10.1175/JHM-D-11-087.1